Hydrology Research

Hydrology Research Vol 52 No 4, 905 doi: 10.2166/nh.2021.014

Analysis of sheet erosion component variability on four complex hillslopes and consecutive storms under laboratory conditions

Mahboobeh Kiani-Harchegani [a,*], Ali Talebi[a] and Sajad Kiani[b]
[a] Department of Watershed Management Engineering, Faculty of Natural Resources, Yazd University, Yazd, Iran
[b] Department of Water and Environmental Engineering, Shahid Chamran University of Ahvaz, Ahvaz, Iran
*Corresponding author. E-mail: mahboobeh.kiyani20@gmail.com

MK, 0000-0003-1075-1169

ABSTRACT

Understanding of rainfall-runoff processes in arid and semi-arid regions, such as runoff discharge (Q) and sediment concentration (SC) in hillslopes with different geometries, can offer better insights into hydrological processes. Consequently, considering intra- and inter-storm dynamics of Q and SC during consecutive storms (CSs), on hillslopes of various geometric shapes, has not been accurately and scientifically studied. The current research was planned to study the response of the sheet erosion components. The experiments were performed on four complex hillslopes (CHs) including straight-parallel, straight-convergent, concave-convergent, and convex-convergent under five CSs with rainfall intensity of 45 mm/h on a sandy loam soil in a 1×2 m^2 plot under laboratory conditions. The results showed that the individual effects of the CSs and CHs and their interactive effects on Q and SC were significant ($P \leq 0.00$). However, Q was more influenced by the CSs ($\eta_p^2 = 0.65$) and SC was more affected by the CHs ($\eta_p^2 = 0.77$). Moreover, analysis of the hydrographs (HGs), sedigraphs (SGs), and sediment rating loops (SRLs) observed in four CHs during five CSs indicated the diversity in the behavior of the SC (from 2.32 to 68.68 g/L) in comparison with variations in Q (from 14.68 to 38.38 mL/s).

Key words: detachment and deposition, hillslope scale, interrill erosion, sediment mobilization, soil loss

HIGHLIGHTS

- Q and SC in different CSs and CHs studied under laboratory conditions.
- Q and SC had significant difference in different CSs and CHs.
- The ηp2-value showed that the Q was more influenced by the CSs and SC was more affected by the CHs.
- The SRLs analysis showed the complexity of the sediment behavior in different CSs and CHs.

INTRODUCTION

Soil erosion and yield sediment are among the most critical environmental problems, especially in arid and semi-arid regions, and play a very important role in water and soil conservation plans, watershed management projects, and development of water resources and dam construction (Sepehri *et al.* 2021). Since soil erosion is a very complex process, and the sediment resulting from it is deposited in the slope failure areas after the detachment and transport processes, understanding the detachment, transport, and deposition processes is key to developing soil erosion models. Therefore, accurate knowledge of the processes governing soil erosion, sediment transport, and their possible interactions is of great importance in developing soil erosion models (Mahmoodabadi & Cerdà 2013; Rodrigo-Comino *et al.* 2016, 2019). In addition, sediments are considered the final result of the soil erosion process and one of the fundamental components of the rainfall-runoff process that exhibit complex temporal and spatial variations on the storm scale. Hence, the study of changes in the sediment load on various scales is considered a necessary undertaking and can be used as an indicator for evaluating and understanding the situation governing the system. Furthermore, correct understanding of hydrological processes in watershed systems and also the conditions governing the hydrological cycle is an unavoidable necessity for the comprehensive soil and water management of watersheds (Sadeghi *et al.* 2019). In this regard, studies on various temporal and spatial scales and accurate analysis of the different components of sediment production processes and factors influencing sediment production have attracted

the attention of researchers. Consequently, extensive studies have been conducted in this area because of the need to know the quantity of the transported sediment load and its temporal and spatial variations (e.g., Rovira & Batalla 2006; Nadal-Romero *et al.* 2008; Sun *et al.* 2016; Sadeghi *et al.* 2019; Haddadchi & Hicks 2021).

The pattern of changes in sediment concentration (SC) during storm events indicates the complex relationship between runoff discharge (Q) and SC that is influenced by various factors. For this purpose, sedigraphs (SGs), which represent temporal distribution or changes of SC during hydrological events, have been used as an important tool to analyze sediment behavior with changes of Q (Saeidi *et al.* 2016), and sediment rating loops (SRLs), which are based on accurate relationship and intra- and inter-storm variability of the studied events, have been employed as a suitable tool to understand the controlling role of Q in sediment production (Mostafazadeh *et al.* 2015; Kiani-Harchegani *et al.* 2018). SRLs are classified based on the relationship between SC and Q in various forms including: (i) single-valued line (for a given Q, the peaks in the SG and in the hydrograph (HG) occur at the same time); (ii) clockwise loop (during a storm event, the peak in the SG happens before that in the HG); (iii) anticlockwise loop (during a storm event, the peak in the SG happens after that of the HG); (iv) the single line plus loop (a combination of the single-valued line and the clockwise loop or the anticlockwise loop); (v) figure eight (that can be in the form of clockwise–anticlockwise loop or first in the form of anticlockwise loop and then in the form of clockwise loop due to the presence and supply of sediment and, hence, increased SC during the storm), and (vi) the complex pattern (a combination of figure eight and clockwise loop or anticlockwise loop) (Williams 1989; Haddadchi & Hicks 2021). Since studies have been conducted on the behavior of and changes in SRLs under various conditions on the watershed scale, and given the very complex natural conditions governing the watersheds, it seems necessary to simplify and control some of the conditions and consider some parameters and study their effects on the behaviors of the mentioned phenomena in order to better understand the erosion soil processes.

The geometry of hillslopes is also one of the important factors in hydrological processes on various temporal and spatial scales. Natural hillslopes in a watershed are not always rectangular with straight curvature and can appear in different shapes. Whether flow lines along the path lines are convergent or divergent is used to classify hillslopes as convergent, divergent, or parallel (Aryal *et al.* 2005). Determination of the effect of these factors is effective in correctly and suitably planning management of water and soil resources and controlling the evolutionary process of soil erosion (Kiani-Harchegani *et al.* 2019). Suitable understanding and feedback between the various shapes of hillslopes and their hydrological processes can be very useful in watershed management (Amanian *et al.* 2018). At present, hydrological models are widely used to better understand the influential factors in the hydrological cycle of the watersheds, and these models have applications in many issues related to management of water resources including rainfall-runoff modeling and sediment management. Consequently, recognition of the geometry of hillslopes is vital for the accurate performance of the various models developed for soil erosion (Sabzevari & Talebi 2019). Various studies have been carried out worldwide on the components of sheet erosion, such as surface runoff and soil loss on complex hillslopes (CHs) (Agnese *et al.* 2007). In this regard, we can mention research by Talebi *et al.* (2008, 2016); Sabzevari *et al.* (2010), Geranian *et al.* (2013), Amanian *et al.* (2018), and Meshkat *et al.* (2019), who studied the effects of CHs including hillslope plan shapes (convergent, divergent, parallel) and their longitudinal profiles (straight, convex, and concave) on the behavior and volume of produced surface and sub-surface runoff and soil loss during the rainfall-runoff process under various laboratory conditions. The results of these studies suggest that dynamic changes happen in surface runoff and soil loss on CHs in various laboratory conditions. However, no study has been conducted on the behavior of surface runoff and SC during consecutive storms (CSs) in CHs.

Considering the many difficulties and the high costs of sampling runoff and sediments resulting from CSs on hillslopes with various shapes on the watershed scale, it is recommended to conduct simulated experiments in the laboratory using rainfall simulators on the scale of laboratory plots. This method is one of the most fundamental tools required for research on the components of the soil erosion process (Parsons & Lascelles 2000). The most important advantage of using a rainfall simulator is that this process is more rapid, efficient, controllable, and flexible than natural rainfall (Meyer & Harmon 1984; Rodrigo-Comino *et al.* 2016; Kiani-Harchegani *et al.* 2019). Therefore, study of changes in the components of soil erosion during CSs on various hillslope shapes under laboratory conditions can help develop soil erosion sciences, understand the various dimensions of temporal intra- and inter-storm variability in the main hydrological processes and prepare the ground for a better understanding of watershed systems, development of more accurate models and, finally, better management of watershed resources. Consequently, the present research was carried out to analyze the components of sheet erosion including Q and SC in four CHs during five CSs in a sandy loam soil taken from the Tahoneh watershed as the sample

watershed in arid regions of Iran. This sample watershed is located in Yazd province with an average slope of 20% at rainfall intensity of 45 mm/h.

MATERIAL AND METHODS

Preparation of laboratory conditions

In this study, the rainfall simulator was set and profile curvature and plan shapes of four CHs were designed at the Hydraulic Laboratory, Department of Civil Engineering, Yazd University, Yazd, Iran. The portable rainfall simulator was used in the experiments (Figure 1). This rainfall simulator with oscillating Veejet 80,100 nozzles produced water drops with the mean diameter of 285 mm at a height of about 3 m and pressure of 55 kPa. The calculated energy for the calculated drop size distribution was 27.10 J/m^2/mm (Jahanbakhshi *et al.* 2018; Kavian *et al.* 2019). Before starting the experiments using the rainfall simulator, rainfall intensity and nozzle angle and oscillating velocity had to be calibrated. To study homogeneity of rainfall intensity, 12 sharp-edged containers with a distance of 50 cm from each other were used to apply rainfall intensity of 45 mm/h employing a graduated cylinder. The volume of water in the cylinder was divided by the area of the container and rainfall intensity was validated. The rainfall intensity of 45 mm/h had acceptable homogeneity with standard deviation of ± 7 mm/h and homogeneity coefficient of 81.20% in the plot (Gabric *et al.* 2014). Thus, the rainfall simulator was set up for a rainfall intensity of 45 $\pm$ 7 mm/h and duration of 15 min in a return period of 25–30 years according to the soil and water conservation activities in watersheds. The characteristics of CSs are according to the intensity–duration–frequency (IDF) curves in the Khezr-Abad climatic station near Tahoneh watershed. Events were created with time intervals of about 3–5 days to generate the antecedent soil moisture (Mahdavi 2002).

Laboratory plot

The present research was conducted on a soil sample taken from an area in the Tahoneh watershed with longitude and latitude of 53° 56′ and 31° 49′, respectively. The soil sample was taken from a depth of 20 cm of the surface layer and transferred to the laboratory where operations such as air drying were performed to enable its moisture content to reach the optimum level. The gravel and plant residues were then removed from the air-dried soil sample, which was sieved using an 8 mm sieve and mixed (Kiani Harchegani *et al.* 2017). Some physical and chemical characteristics of the soil sample which were measured are briefly listed in Table 1. Prior to moving the soil sample to the plot, a drainage layer consisting of mineral aggregates with a gradual change in particle size from almond to fine-grained particles was poured from the bottom of the plot to a height of about 20 cm (Khaledi Darvishan *et al.* 2014).

The experiments were performed at a 20% slope on concave, convex, and straight longitudinal profiles and parallel and convergent plan shapes. The straight-parallel plot (2 m long and 1 m wide) was first designed and five CSs were applied. Hillslopes with straight-convergent, concave-convergent, and convex-convergent geometries in the 2 m by 1 m plot were designed

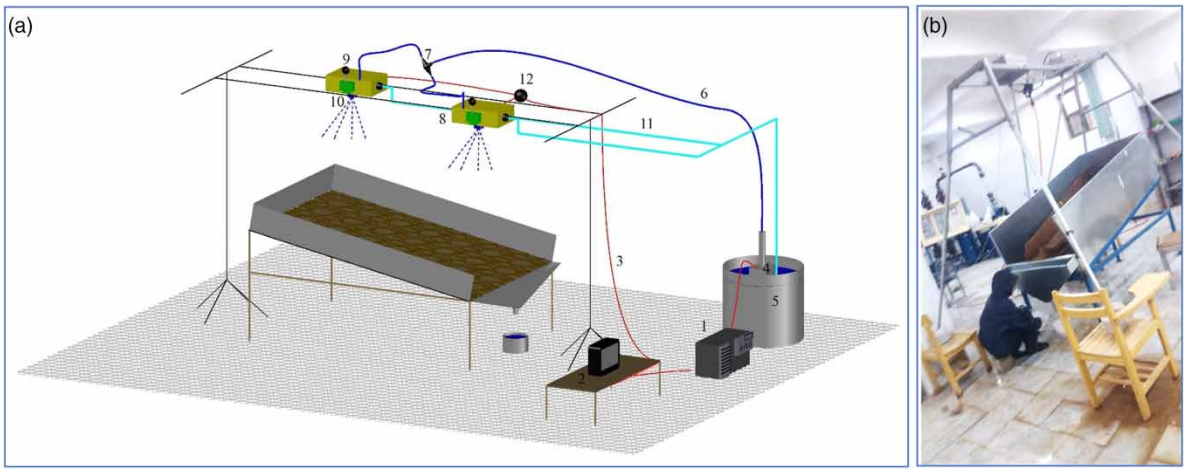

Figure 1 | (a) Schematic diagram of laboratory setup used in the present study including rainfall simulator (1. electric generator, 2. control board, 3. cable, 4. electric pump, 5. water tank, 6. water transfer hose, 7. three-way water divide, 8. control box, 9. manometer, 10. swinging nozzle, 11. bypass tube, and 12. power distribution box) and plot; (b) experimental setup in the Hydraulic Laboratory.

Table 1 | Some of the physical and chemical properties of the soil used in the laboratory

Parameter	EC (dS/m)	pH	Total nitrogen (%)	Organic carbon (%)	Total neutralizing value (%)	Sand (%)	Silt (%)	Clay (%)	Texture
Value	1.7	7.8	0.01	0.01	26.5	62	26	12	Sandy loam

using plexiglass sheets for the convergent plan and mineral aggregate for the concave and convex plan (Figure 1). According to Figure 2 and Table 2, the length and width of the plot were calculated using Equations (1)–(3) and utilizing plexiglass sheets and the profile elevation employing mineral aggregate for the various types of CHs including straight-parallel, straight-convergent, concave-convergent, and convex-convergent and implemented on the 2 m by 1 m plot (Talebi *et al.* 2008; Meshkat *et al.* 2019).

$$z(x, y) = E + H\left(1 - \frac{x}{L}\right)^n + \omega y^2 \tag{1}$$

$$w(x) = c_w \exp\left\{c_s\left(1 - \frac{x}{L}\right)^{2-n}\right\} \tag{2}$$

$$c_s = \frac{2\omega L^2}{n(2-n)H} \tag{3}$$

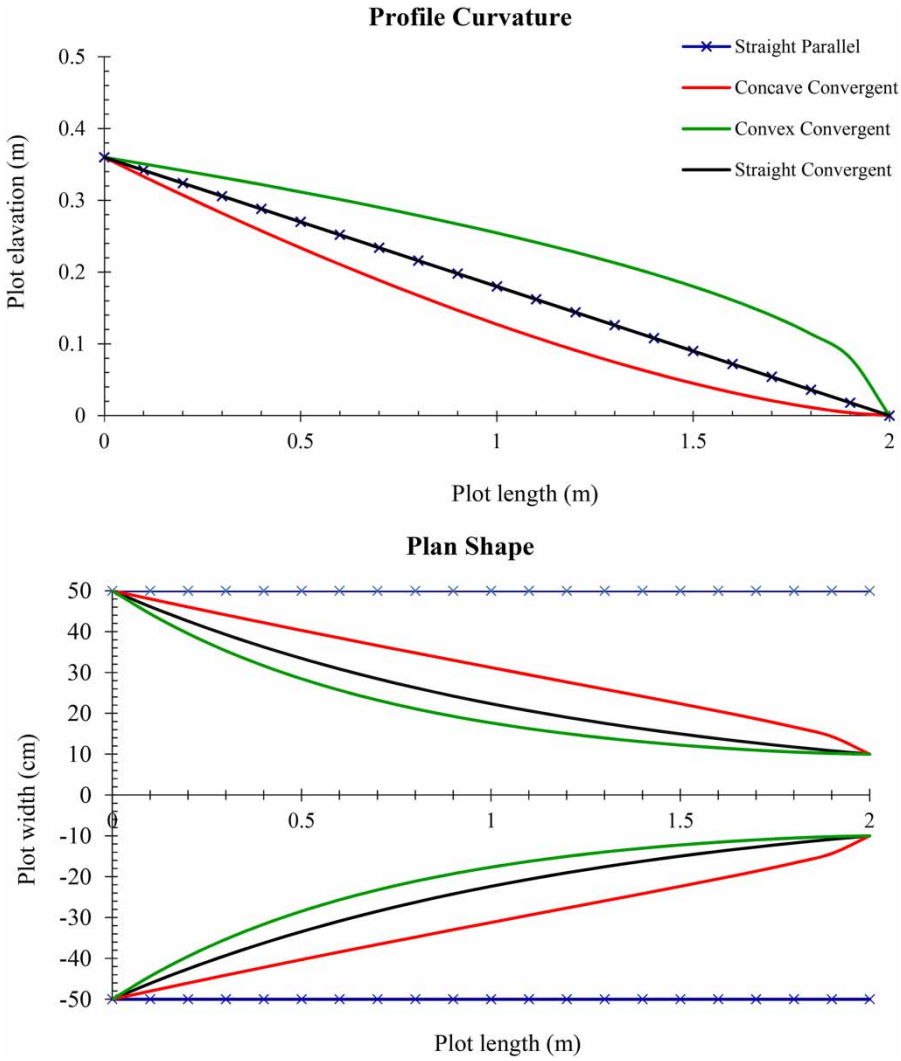

Figure 2 | Profile curvature and plan shape of four CHs in a 1 × 2 m^2 plot.

Table 2 | Geometric properties of the four CHs used in this study

No.		Longitudinal profile	Plan shape	H (m)	N (no. dimension)	L (m)	ω (m^{-1})
1		Straight	Parallel	0.36	1	2	0.0000
2		Straight	Convergent	0.36	1	2	± 0.0997
3		Concave	Convergent	0.36	1.5	2	± 0.0997
4		Convex	Convergent	0.36	0.5	2	± 0.0997

where z, x, and y are the elevation, the horizontal distance in the direction of the length of hillslope towards the end of the basin, and the horizontal distance from the center of the gradient in the vertical direction towards the length of the hillslope, respectively. E and H are the minimum and maximum heights relative to the baseline, respectively. L is the length of the hillslope in meters, and n is the profile curvature parameter which has no dimension, ω is the plan shape parameter, c_w defines the width of the hillslope at the outlet (x = L), c_s defines the degree of topographic convergence (Talebi *et al.* 2008, 2016).

After preparing the hillslope plan and longitudinal profile in the plot, a hemp sack was first placed on the mineral aggregate and the soil sample was poured into the plot in two 5-cm layers and rolled to reach the specific density of the soil in the sampling area. After pouring in the first layer, the soil was scratched transversely to prevent a gap forming between the first and second layers (Kiani Harchegani *et al.* 2016). The experiments were designed in three series. After each series, the soil in the plot was completely removed, the hemp sacks were replaced, and the initial conditions in the plot were recreated to perform the next series of experiments.

Measurements of Q and SC

The time when the first signs of runoff and sediment appeared in the outlet of the plot, it was recorded using a chronometer and runoff volume was measured at 1-min intervals using 1-liter beakers. Then, the SC in sheet erosion was determined using the decantation method for 24 h, emptying the supernatant, and drying the sediment in an oven at 105 °C (Kiani-Harchegani *et al.* 2018).

Data analysis

The databank for the data was obtained from Q and SC resulting from sheet erosion during the five CSs with rainfall intensity of 45 mm/h at 1-min intervals in four CHs with different geometric shapes in Excel 2016. Duncan's test was used for grouping inter-storm variations in the mean values of Q and SC. Also, the effect of CHs and CSs and their interaction on Q and SC was investigated using two-way ANOVA in the IBM SPSS Statistics 26 software (IBM, USA). Finally, HGs, SGs, and SRLs were prepared and analyzed during the five CSs in four CHs (Kiani-Harchegani *et al.* 2018, 2019).

RESULTS AND DISCUSSION

Intra- and inter-storm variation of Q and SC during CSs in CHs

The results related to intra-storm variations in Qs and SCs resulting from five CSs at 20% slope and rainfall intensity of 45 mm/h on straight-parallel, straight-convergent, concave-convergent, and convex-convergent hillslopes are presented in Figures 3 and 4. Moreover, results obtained from the inter-storm variations of them are listed in Table 3. Results of Figure 3 demonstrate that on various hillslopes the Qs in the first event had greater intra-storm variations compared to the other events. These results are in line with those of Hu *et al.* (2016) about unsteady runoff during the first few minutes of the first storm due to variations in surface storage. Nevertheless, inter-storm variations, according to the results presented in Table 3, in mean Qs in the first event were the smallest compared to the following CSs. The mean Qs on the concave-convergent, straight-parallel, convex-convergent, and straight-convergent hillslopes with the values of 14.68, 16.92, 18.49, and 18.67 mL/s in the first event were significantly different ($P \leq 0.00$) to the mean values of the Q in the second to fifth events.

The results listed in Figure 4 show that SC had a more complex behavior than Q. These results conform to the findings by Nearing *et al.* (1999), Bagarello & Ferro (2004), and Kiani-Harchegani *et al.* (2018) concerning the behavioral complexities due to various movement patterns of sediment particles and the detachment processes and deposition proportionate to

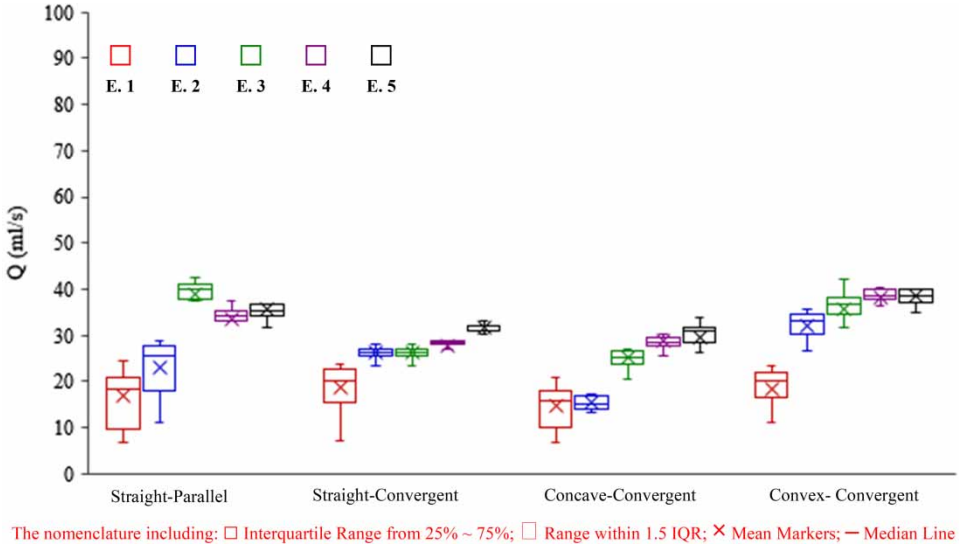

Figure 3 | Box plots of intra-storm variation of Q during five CSs in four CHs.

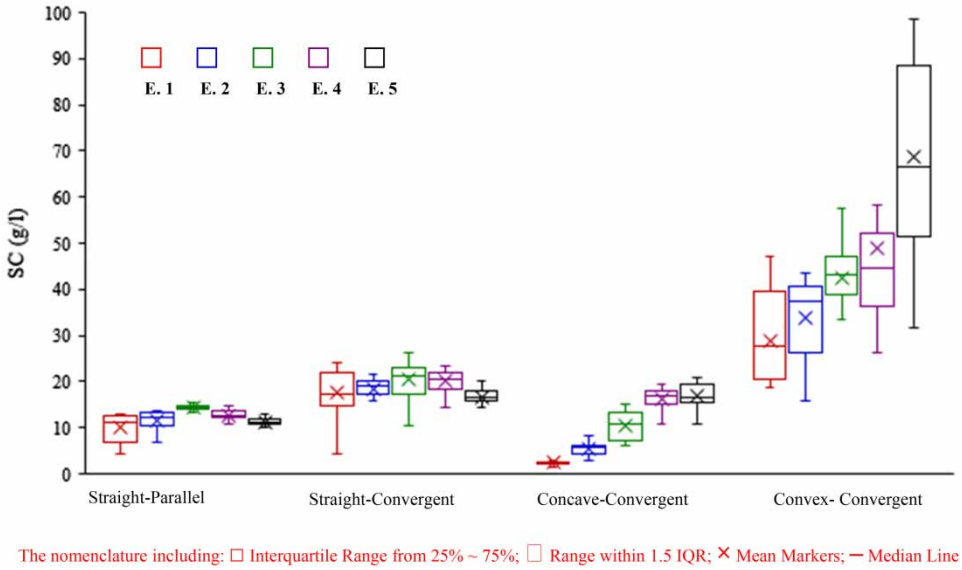

Figure 4 | Box plots of intra-storm variation of SC during five CSs in four CHs.

particle size of sediment. Figure 4 indicates very little intra-storm variation in SC on the straight-parallel hillslope from the third to the fifth events. Furthermore, based on the results in Table 3, the mean SCs in the third, fourth, and fifth events on the straight-parallel hillslope were not significantly different ($P \geq 0.05$). However, as shown in Figure 4, intra-storm variations in SC in the third event were greater compared to the first and second events on straight-convergent, concave-convergent, and convex-convergent hillslopes. In addition, a close look at Table 3 reveals that the trends of variations in the mean values of SC on straight-parallel and straight-convergent were similar. SCs in the fourth and fifth events on these hillslopes were less compared to the third event whereas on concave-convergent and convex-convergent hillslopes the increasing trend in variations continued. Based on results reported by Geranian *et al.* (2013) and Meshkat *et al.* (2019), parallel hillslopes exhibited almost constant variations in the components of sheet erosion considering their constant upstream and downstream width; whereas, on convergent hillslopes, variations in SC still increased with the passage of time because of the greater upstream area compared to the downstream area. In the study of the profiles of the hillslopes also,

Table 3 | Results of inter-storm of Q (mL/s) and SC (g/L) during CSs on CHs using Duncan's test

CHs	Variables	CSs				
		E 1 Mean ± S.D.	E 2 Mean ± S.D.	E 3 Mean ± S.D.	E 4 Mean ± S.D.	E 5 Mean ± S.D.
Straight-parallel	Q	16.92 ± 6.32 c	23.39 ± 6.11 b	35.93 ± 8.99 a	33.94 ± 3.57 a	35.14 ± 3.81 a
	SC	10.05 ± 3.17 c	11.47 ± 2.040 bc	14.28 ± 1.03 a	12.72 ± 1.08 b	11.25 ± 1.36 bc
Straight-convergent	Q	18.67 ± 5.16 c	25.69 ± 3.02 b	26.21 ± 3.01 b	27.83 ± 2.51 b	31.67 ± 3.60 a
	SC	17.58 ± 5.44 b	18.27 ± 2.85 abc	20.43 ± 4.055 a	19.95 ± 2.35 bc	16.36 ± 2.07 c
Concave-convergent	Q	14.68 ± 4.53 c	15.59 ± 4.37 c	25.34 ± 4.56 b	28.75 ± 4.00 a	29.71 ± 3.30 a
	SC	2.32 ± 0.32 d	5.21 ± 1.29 c	10.27 ± 3.35 b	16.33 ± 2.24 a	16.99 ± 2.63 a
Convex-convergent	Q	18.49 ± 5.37 c	31.95 ± 2.52 b	35.84 ± 2.57 a	38.33 ± 1.34 a	38.38 ± 2.27 a
	SC	28.76 ± 9.99 d	33.76 ± 7.93 cd	42.56 ± 6.27 bc	48.98 ± 19.83 b	68.68 ± 18.30 a

concave profiles, because of their lower slope at the end of the plot, could be a site for storage and accumulation of surface runoff and sediment deposition compared to the other profiles. Consequently, the mean of Q and SC on the concave-convergent hillslope were lower compared to the other hillslopes, especially in the first event. However, the mean of Qs and SCs were lower on the straight profile compared to the hillslopes with convex profile because the slopes were more uniform at the beginning and end of the plot in straight profile. These results agree with those found by Sabzevari & Talebi (2019) concerning the high values of SC on convex hillslopes compared to straight and concave ones.

Effect of CSs and CHs and their interaction on Q and SC

The results obtained from the effects of five CSs and four CHs (straight-parallel, straight-convergent, concave-convergent, and convex-convergent) and their interactive effects on the components of sheet erosion (Q and SC) using two-way ANOVA at a confidence interval of 95% are presented in Table 4. As shown by the results in Table 4, the individual and interactive effects of CSs and CHs on Q and SC were significant ($P \leq 0.00$). Consequently, the partial eta-squared statistic (η_p^2) was also used to study the extent of their effects on Q and SC (Kiani-Harchegani *et al.* 2019). The results indicated that Q was influenced about 1.58 times more by the CSs ($\eta_p^2 = 0.65$) than by the CHs ($\eta_p^2 = 0.41$). These results are in agreement with the findings of dos Santos *et al.* (2017) and Gholami *et al.* (2019), that there was a positive correlation between Q and rainfall events. Moreover, the results revealed that the effects of various CHs shapes ($\eta_p^2 = 0.77$) on SC were 2.56 times greater than those of the CSs ($\eta_p^2 = 0.30$). These results conform to the finding of Talebi *et al.* (2016) that the geometry of CHs influenced sheet erosion processes, especially variations in detachment and sediment deposition, compared to rainfall events. Study of the interactive effects of different CHs and CSs on Q and SC also, shown in Table 4, indicate that there were significant differences ($P \leq 0.00$) between their mean values under different conditions, but the ηp^2 value showed that these two factors had noninteraction effects on Q and SC (0.21 and 0.38, respectively).

HGs, SGs, and SRLs during CSs in CHs

The results obtained from the analysis of the HGs, the SGs, and SRLs of the five CSs on the straight-parallel, straight-convergent, concave-convergent, and convex-convergent hillslopes at rainfall intensity of 45 mm/h are shown in Figures 5 and 6, respectively.

Table 4 | Effect of CHs and CSs and their interaction on Q (mL/s) and SC (g/L) using two-way ANOVA in GLM

Characteristics	Factors	df	Mean square	F-value	*P*-value	Partial eta squared (η_p^2)
Q	CHs	3	1,230.17	60.57	0.00	0.41
	CSs	4	2,535.67	124.85	0.00	0.65
	CHs × CSs	12	121.29	5.97	0.00	0.21
SSC	CHs	3	17,577.38	299.28	0.00	0.77
	CSs	4	1,672.42	28.47	0.00	0.30
	CHs × CSs	12	795.38	13.54	0.00	0.38

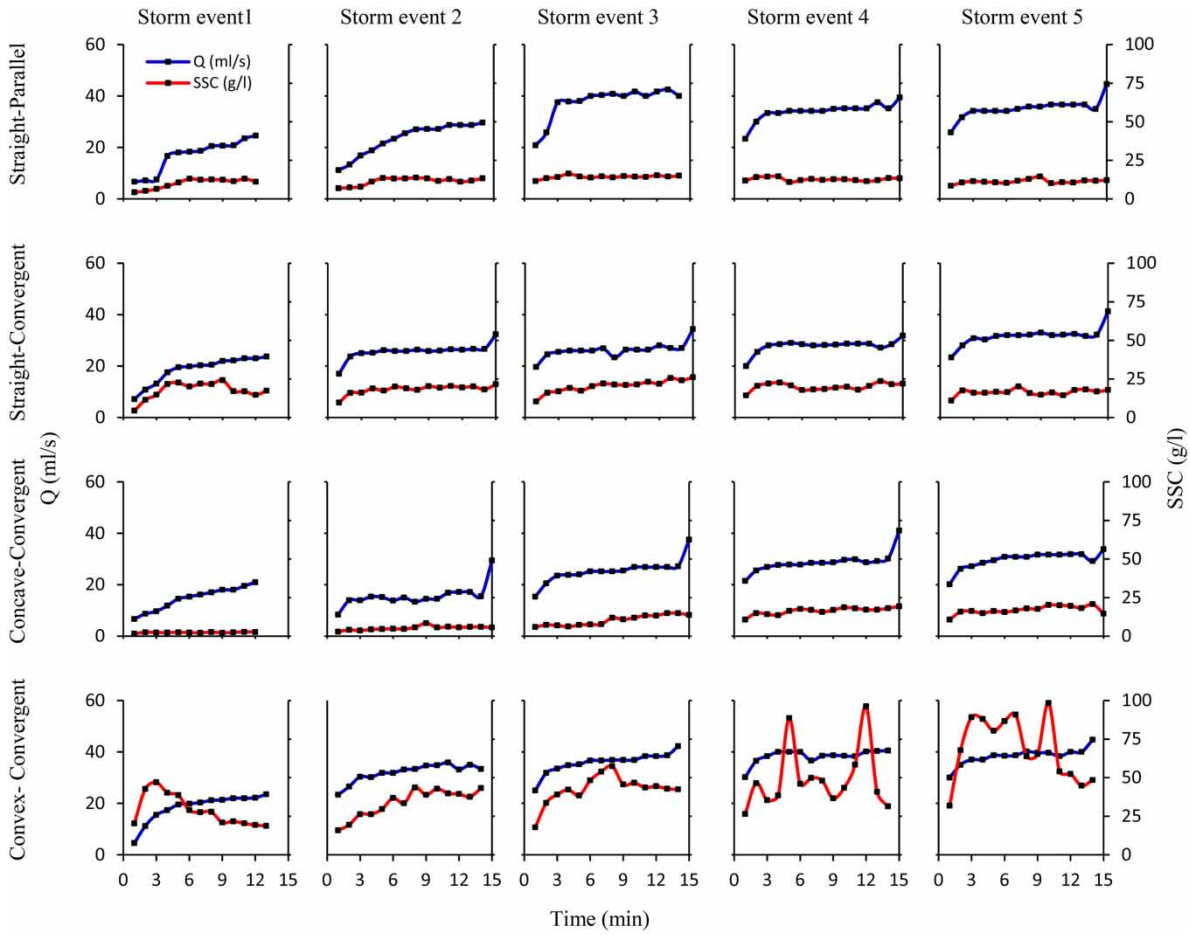

Figure 5 | HGs and SGs during five CSs in four CHs.

The results related to the HGs and SGs in Figure 5 indicate unsteady state runoff in the beginning minutes of the HG, that changed to the steady state later. This conforms to the findings of Gholami *et al.* (2019) concerning the effect of the initial moisture in the soil during the first few minutes of the storm event resulting in an increase in runoff infiltration into the soil and then into the steady-state runoff flow when the steadier state in the infiltration process was achieved. Furthermore, the SGs of the five CSs on the straight-parallel, straight-convergent, concave-convergent, and convex-convergent hillslopes show that there were Q–SC regression relationships with coefficients of determination of more than 0.76, 0.70, 0.30, and 0.88 for the first and second storms, respectively. As shown in the figure, the value of the coefficient of determination for the Q–SC regression relationship on the concave-convergent hillslope was low. This agrees with the statement by Geranian *et al.* (2013), that accumulation of surface runoff at the end of the concave-convergent hillslopes that resulted in sediment deposition was the reason for the low value of the coefficient of determination. Lower values of the coefficient of determination were observed for the third to fifth storms that showed there were weaker relationships between Q and SC due to the complex behaviors of the sediment particles during the detachment, deposition, and transport processes (Kiani-Harchegani *et al.* 2019; Sadeghi *et al.* 2019).

The results related to the SRLs for the five CSs on the four different geometries of CHs in Figure 6 demonstrate diversity in the behavior of the outgoing sediment compared to the changes in Q in the form of the various shapes of the SRLs including clockwise, anticlockwise, composite, and a combination of them. In this regard, in the first of the five CSs, and in the various shapes of the CHs studied in the present research, the clockwise loop pattern was observed with a rapid sediment discharge compared to Q that showed the effect of the process of particle detachment during the process of splash erosion on provision of sediment that could be transported along the plot. In the second event also, the clockwise SRLs pattern was observed on all

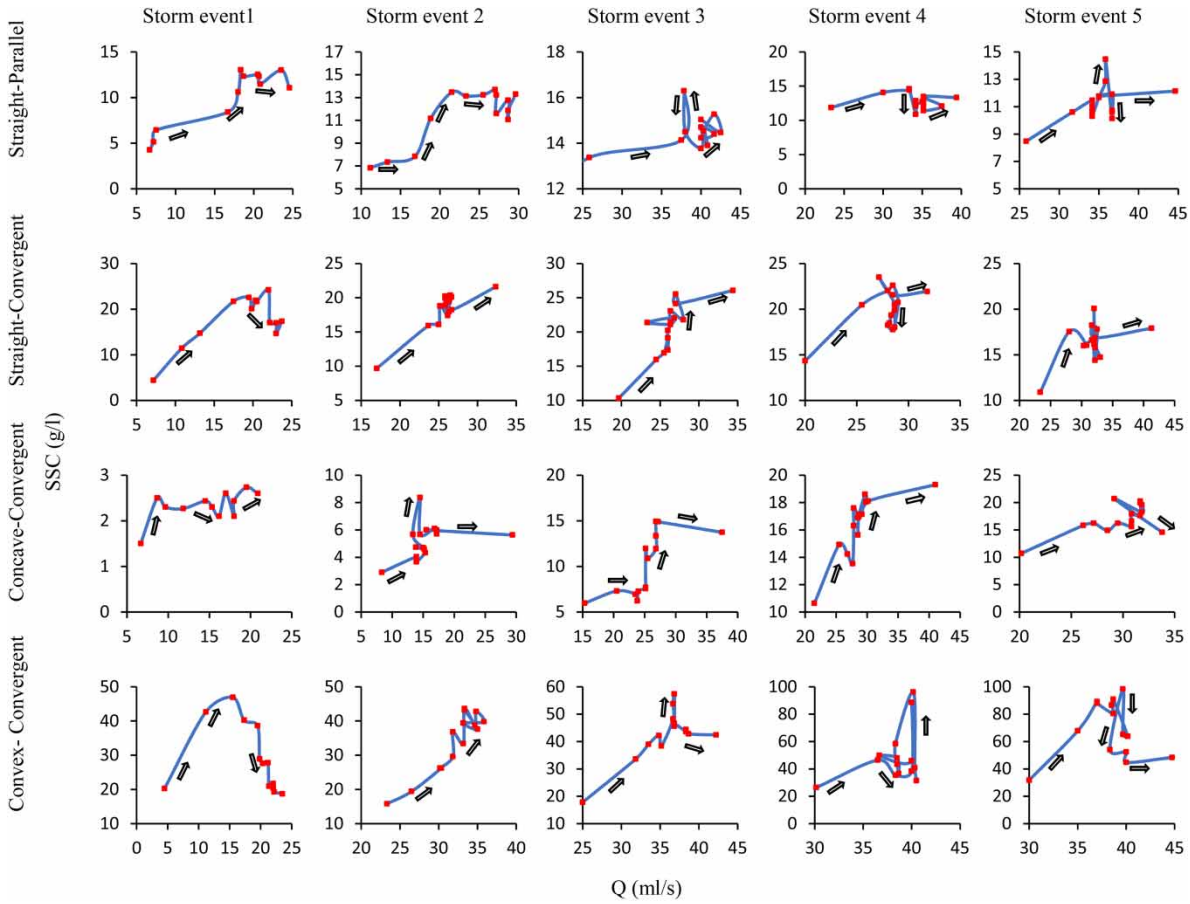

Figure 6 | SRLs during five CSs in four CHs.

the CHs except for the concave-convergent one that indicated the exit of the sediment resulting from the previous events that was deposited near the plot outlet causing its rapid discharge to the plot outlet (Mostafazadeh *et al.* 2015; Sadeghi *et al.* 2019).

In the third event, the increase in the amount of SC leaving the plot outlet on the various CHs led to formation of the figure eight (clockwise-anticlockwise) SRL that showed the increase in SC was more rapid than that in Q, as a result of which, the peak in the SG occurred earlier than that in the HG leading to the formation of the clockwise loop. Following that, due to the presence of sufficient sediment, its transport rate was still high and decreased gradually compared to the HG with the passage of time resulting in the formation of the anticlockwise loops (Saeidi *et al.* 2016).

In the fourth and fifth events on the various CHs, a more complex behavior of SRLs was observed (Figure 6). This was influenced by the participation of different sediment particle size classes that could be attributed to the selective process governing the process during the process of sheet erosion and, hence, transport of sediment particles with various sizes and the change in the weight of the transported sediment, and also to the complex behavior of the sediment under the influence of the consecutive rainfall events. These results are in agreement with the findings of Nadal-Romero *et al.* (2008) and Kiani-Harchegani *et al.* (2018) in this relation. However, based on the results shown in Table 3 and Figure 4, the mean values of SC in the fourth and fifth events on the straight-parallel and straight-convergent hillslopes decreased compared to the previous events and emphasized the lack of sediment caused by the discharge of the sediment produced during the previous events and the increase in the ability of the runoff in transporting the sediment to the plot outlet. These results agree with the findings of Walling & Webb (1982) and Mostafazadeh *et al.* (2015) concerning the controlling role that the presence of sediment had on the shape of the SG. The results also indicated the role of CSs in reducing the total weight of the sediment transported by the storm events. These results are in agreement with the findings of Nadal-Romero *et al.* (2008) and Mostafazadeh *et al.* (2015). However, on hillslopes with concave and convex profiles in the fourth and fifth events the mean values of SC continued to increased compared to the previous events and formed more complex SRLs than the hillslopes with straight profile. This

emphasized the importance of knowing and considering the geometry of CHs in the various hydrological processes and their different effects on the behavior of the components resulting from soil erosion (Talebi *et al.* 2016; Sabzevari & Talebi 2019).

CONCLUSIONS

Analysis of SRLs can have a substantial effect on achieving reliable results to better and more suitably manage water and soil resources, especially proportionate to the temporal scales. Consequently, considering the many difficulties and the high cost of taking Q and SC samples at storm event scales in watershed, simulation experiments were carried out in the laboratory using a rainfall simulator to better understand the relationship between Q and SC and the resulting SRLs and the factors influencing their complex behaviors. In this regard, analysis of the intra- and inter-storm behavior of Q and SC and also SRLs were investigated during the five CSs on four CHs with straight-parallel, straight-convergent, concave-convergent, and convex-convergent geometries. The results indicated that SC was more influenced by the geometry of the hillslopes than the CSs and changes in SRLs were affected by the presence of sediment, the size of sediment particles, and the sediment connectivity processes during the evolutionary processes of erosion. However, study of the behavior of Q suggested that it was more influenced by CSs so that the mean Qs in the fourth and fifth events were higher than those of the events preceding them. Consequently, we can emphasize development of management strategies for suppressing the process of soil erosion proportionate to the geometries of the hillslopes from the first time and location of rainfall on the watersheds. However, it is necessary to conduct complementary research to perform more accurate analyses and complementary summations on other geometries of CHs, especially those with divergent plans.

ACKNOWLEDGEMENTS

The present study has been prepared during the postdoctoral period of the corresponding author at Yazd University. The authors wish to thank Yazd University for its supports of this research (Project No. 97.50.2374). The authors also would like to give thanks to Dr Amanian and En. Zareian for providing facilities at Hydraulic Laboratory and valuable cooperation of En. Asgari in conducting experiments.

DATA AVAILABILITY STATEMENT

Data cannot be made publicly available; readers should contact the corresponding author for details.

REFERENCES

Agnese, C., Baiamonte, G. & Corrao, C. 2007 Overland flow generation on hillslopes of complex topography: analytical solutions. *Hydrological Processes* **21** (10), 1308–1317.

Amanian, N., Geranian, M., Talebi, A. & Hadian, M. R. 2018 The effect of plan and slope profile on runoff initiation threshold. *Watershed Management Science of Engineering* **11** (39), 105–108. (In Persian).

Aryal, S. K., O'Loughlin, E. M. & Mein, R. G. 2005 A similarity approach to determine response times to steady-state saturation in landscapes. *Advances in Water Resources* **28** (2), 99–115.

Bagarello, V. & Ferro, V. 2004 Plot-scale measurement of soil erosion at the experimental area of Sparacia (southern Italy). *Hydrological Processes* **18** (1), 141–157.

dos Santos, J. C. N., de Andrade, E. M., Medeiros, P. H. A., Guerreiro, M. J. S. & de Queiroz Palácio, H. A. 2017 Effect of rainfall characteristics on runoff and water erosion for different land uses in a tropical semiarid region. *Water Resources Management* **31** (1), 173–185.

Gabric, O., Prodanovic, D. & Plavsic, J. 2014 Uncertainty assessment of rainfall simulator uniformity coefficient. *Journal of Faculty of Civil Engineering* 661–667.

Geranian, M., Amanian, N., Talebi, A., Hadian, M. R. & Zeini, M. 2013 Laboratorial investigation of effect of plan shape and profile curvature on variations of surface flow in complex hillslopes. *Iran-Water Resources Research* **9** (2), 64–72. (In Persian).

Gholami, L., Kavian, A., Khaledi Darvishan, A., Alipour, A. & Besarand, Z. 2019 The effect of rainfall pattern on changes of time to runoff and runoff coefficient at plot scale. *Watershed Engineering and Management* **10** (4), 516–528. (In Persian).

Haddadchi, A. & Hicks, M. 2021 Interpreting event-based suspended sediment concentration and flow hysteresis patterns. *Journal of Soils and Sediments* **21** (1), 592–612.

Hu, Y., Fister, W. & Kuhn, N. J. 2016 Inherent interreplicate variability during small-scale rainfall simulations. *Journal of Soils and Sediments* **16** (6), 1809–1814.

Jahanbakhshi, F., Ekhtesasi, M. R., Talebi, A. & Piri, M. 2018 Investigation of sediment production and runoff generation on rock formations of Shirkooh slopes of Yazd using a rainfall simulator. *Journal of Water and Soil Science (Science and Technology of Agriculture and Natural Resources)* **22** (2), 287–299.

Kavian, A., Mohammadi, M., Cerdà, A., Fallah, M. & Gholami, L. 2019 Design, manufacture and calibration of the SARI portable rainfall simulator for field and laboratory experiments. *Hydrological Sciences Journal* **64** (3), 350–360.

Khaledi Darvishan, A., Sadeghi, S. H. R., Homaee, M. & Arabkhedri, M. 2014 Measuring sheet erosion using synthetic colorcontrast aggregates. *Hydrological Processes* **28** (15), 4463–4471.

Kiani Harchegani, M., Sadeghi, S. H. R. & Asadi, H. 2016 Comparative analysis of the effects of rainfall intensity and experimental plot slope on raindrop impact induced erosion (RIIE). *Journal of Soil and Water Research* **46** (4), 631–640. (In Persian).

Kiani Harchegani, M., Sadeghi, S. H. R. & Asadi, H. 2017 Inter-storm variability of coefficient of variation of runoff volume and soil loss during rainfall and erosion simulation replicates. *Ecohydrology* **4** (1), 191–199. (In Persian).

Kiani-Harchegani, M., Saeidi, P. & Sadeghi, S. H. R. 2018 Analysis of rating loops of interrill erosion on consecutive storms under laboratory conditions. *Soil and Water Research* **49** (2), 293–302.

Kiani-Harchegani, M., Sadeghi, S. H., Singh, V. P., Asadi, H. & Abedi, M. 2019 Effect of rainfall intensity and slope on sediment particle size distribution during erosion using partial eta squared. *Catena* **176**, 65–72.

Mahdavi, M. 2002 *Applied Hydrology*, Vol. 2. Tehran University Press, Tehran, Iran, p. 437. (In Persian).

Mahmoodabadi, M. & Cerdà, A. 2013 WEPP calibration for improved predictions of interrill erosion in semi-arid to arid environments. *Geoderma* **204–205**, 75–83.

Meshkat, M., Amanian, N., Talebi, A., Kiani-Harchegani, M. & Rodrigo-Comino, J. 2019 Effects of roughness coefficients and complex hillslope morphology on runoff variables under laboratory conditions. *Water* **11** (12), 2550.

Meyer, L. D. & Harmon, W. C. 1984 Susceptibility of agricultural soils to interrill erosion. *Soil Science Society of America* **48**, 1152–1157.

Mostafazadeh, R., Sadeghi, S. H. R. & Saddodin, A. 2015 Analysis of storm-wise sedimentgraphs and rating loops in Galazchai watershed, West-Azerbaijan. *Soil and Water Conservation Researches* **21** (5), 175–190.

Nadal-Romero, E., Latron, J., Marti-Bono, C. & Regues, D. 2008 Temporal distribution of suspended sediment transport in a humid Mediterranean badland area: the Araguas catchment, Central Pyrenees. *Geomorphology* **97** (3–4), 601–616.

Nearing, M. A., Govers, G. & Norton, L. D. 1999 Variability in soil erosion data from replicated plots. *Soil Science Society of America Journal* **63** (6), 1829–1835.

Parsons, A. J. & Lascelles, B. 2000 Rainfall simulation in geomorphology. *Earth Surface Processes and Landforms* **25** (7), 679–689.

Rodrigo-Comino, J., Sinoga, J. R., González, J. S., Guerra-Merchán, A., Seeger, M. & Ries, J. B. 2016 High variability of soil erosion and hydrological processes in Mediterranean hillslope vineyards (Montes de Málaga, Spain). *Catena* **145**, 274–284.

Rodrigo-Comino, J., Senciales, J. M., Sillero-Medina, J. A., Gyasi-Agyei, Y., Ruiz-Sinoga, J. D. & Ries, J. B. 2019 Analysis of weather-type-induced soil erosion in cultivated and poorly managed abandoned sloping vineyards in the Axarquía Region (Málaga, Spain). *Air, Soil and Water Research* **12**, 1178622119839403.

Rovira, A. & Batalla, R. 2006 Temporal distribution of suspended sediment transport in a Mediterranean basin: the Lower Tordera (NE SPAIN). *Geomorphology* **79**, 58–71.

Sabzevari, T., Talebi, A., Ardakanian, R. & Shamsai, A. 2010 A steady-state saturation model to determine the subsurface travel time (STT) in complex hillslopes. *Hydrology and Earth System Sciences* **14** (6), 891–900.

Sabzevari, T. & Talebi, A. 2019 Effect of hillslope topography on soil erosion and sediment yield using USLE model. *Acta Geophysica* **67** (6), 1587–1597.

Sadeghi, S. H. R., Saeidi, P., Singh, V. P. & Telvari, A. R. 2019 How persistent are hysteresis patterns between suspended sediment concentration and discharge at different timescales? *Hydrological Sciences Journal* **64** (15), 1909–1917.

Saeidi, P., Sadeghi, S. H. R. & Telvari, A. R. 2016 Simulation of sediment graph using hydrograph. *Journal of Watershed Engineering and Management* **8** (1), 28–41.

Sepehri, M., Ghahramani, A., Kiani-Harchegani, M., Ildoromi, A. R., Talebi, A. & Rodrigo-Comino, J. 2021 Assessment of drainage network analysis methods to rank sediment yield hotspots. *Hydrological Sciences Journal* **66**, 904–918.

Sun, L., Yan, M., Cai, Q. & Fang, H. 2016 Suspended sediment dynamics at different time scales in the Loushui River, south-central China. *Catena* **136**, 152–161.

Talebi, A., Troch, P. A. & Uijlenhoet, R. 2008 A steady-state analytical slope stability model for complex hillslopes. *Hydrological Processes* **22** (4), 546–553.

Talebi, A., Hajiabolghasemi, R., Hadian, M. R. & Amanian, N. 2016 Physically based modelling of sheet erosion (detachment and deposition processes) in complex hillslopes. *Hydrological Processes* **30** (12), 1968–1977.

Walling, D. E. & Webb, B. W. 1982 Sediment availability and the prediction of storm-period sediment yields. In *Recent Developments in the Explanation and Prediction of Erosion and Sediment Yield, Proceedings of the Exeter Symposium July 1982*, Vol. 137. IAHS Publication, pp. 327–337.

Williams, G. P. 1989 Sediment concentration versus water discharge. *Journal of Hydrology* **111**, 89–106.

First received 14 February 2021; accepted in revised form 16 May 2021. Available online 10 June 2021